Supporting Information

for

Direct EPR Observation of a Tyrosyl Radical in a Functional Oxidase Model in Myoglobin during both H_2O_2 and O_2 Reactions

Yang Yu,[†∓] Arnab Mukherjee,[‡∓] Mark J. Nilges,[¶] Parisa Hosseinzadeh,[§] Kyle D. Miner[§] and Yi Lu[*, †, ‡, §]

[†]Center for Biophysics and Computational Biology, [‡]Department of Chemistry and [§]Department of Biochemistry and [¶]The Illinois EPR Research Center, University of Illinois at Urbana–Champaign, Urbana, Illinois 61801, United States

Experimental:

All chemicals were purchased from Sigma with reagent grade or higher, and used without further purification. WT Mb, Cu_BMb,F33Y-Cu_BMb and F33Y/Y103F/Y146F/Y151F-Cu_BMb were expressed and purified according to previously reported method and verified by ESI-MS. [1,2]

Myoglobin and mutants in 100 mM potassium phosphate buffer were concentrated to 0.25mM by ultrafiltration using Amicon Ultra® (Millipore, Billerica, MA). Glycerol (50 µL) was added into 200 µL of protein as glassing agent. 250 µL of the protein solution was loaded into EPR tube and flash-freeze in liquid nitrogen as untreated sample. Myoglobin and mutants were reacted with H_2O_2 by adding 2.5 µL of 20 mM H_2O_2 (one equivalence) into 250 µL of the protein solution and flash-freezing after 30 s of mixing.

To prepare samples of ferrous F33Y-Cu_BMb for reaction with O_2, ferric F33Y-Cu_BMb(~0.5 mM) was reduced by sodium dithionite inside glove bag and subsequently passed through a short Sephadex® G-25 column to remove unreacted dithionite. Ferrous F33Y-Cu_BMb was transferred into a syringe and sealed inside glove bag. The syringe was transferred outside for rapid freeze-quench. Potassium phosphate buffer(100 mM, pH 7) containing 10% glycerol was purged with O_2 for 20 min. The O_2 saturated solution was transferred into another syringe.

Rapid freeze-quench was performed at 25 °C, using an Update Instruments System 1000 equipped with a Wiskind Grid Mixer, a spraying nozzle, and a stirred isopentane bath, cooled by liquid nitrogen to approximately -130 °C. Ferrous F33Y-Cu_BMb and O_2 saturated buffer containing 10% glycerol was mixed and passed through a delay hose of appropriate length to give the desired quench time (~20 ms). The sample was frozen by spraying into approximately -130 °C spectrophotometric grade isopentane in a Pyrex collection funnel attached to the EPR tube. A pre-cooled packing rod and syringe were used to pack the frozen powder to the bottom of EPR tube, while the whole set-up was kept in isopentane bath. After packing, EPR samples were stored in liquid nitrogen for less than two days before data were collected.

X-band EPR spectra were collected on a Varian E-122 spectrometer at the Illinois EPR Research Center (IERC). The samples were run at ∼30 K using liquid He and an Air Products Helitran cryostat with 20% glycerol. Magnetic fields were calibrated with a Varian NMR gaussmeter, and the frequencies were measured with an EIP frequency counter. Based on power saturation experiment (Figure S8) and spectra taken at various temperature (Figure S9), the typical power (2 mW) and temperature (30 K) used in measurement did not saturate spectra. Q-band EPR spectra were collected on a Bruker ElexSys E-580 spectrometer equipped with an ER 5106 QT probe.

Concentration of tyrosyl radical was quantified by spin counting with (2,2,6,6-Tetramethylpiperidin-1-yl)oxy (TEMPO) as standard. TEMPO was dissolved in water to afford a 0.1M stock solution. A series of standard solution of TEMPO were diluted from stock solution with concentration spanning 0-1 mM. EPR signal was integrated. Concentration of radical from H_2O_2 reacted F33Y-Cu_BMb was calculated based on TEMPO standard curve.

EPR spectra were simulated with SIMPOW6.[3]

EPR spectra of various power were recorded to determine power saturation properties of tyrosyl radical. The data were fitted with the equation [4]:

$$S = k \times \sqrt{P}/[1 + (2^{2/b} - 1)(P/P_{1/2})]^{b/2}$$

In the equation, S is the signal strength integrated from EPR spectra; k is a constant depends on experiment setup; P is the microwave power; $P_{1/2}$ is the microwave power where the first-derivative amplitude is reduced to one-half of its unsaturated value; b is the relaxation factor where b equals to 1 for inhomogeneous line broadening and b equals to 3 for homogeneous line broadening.

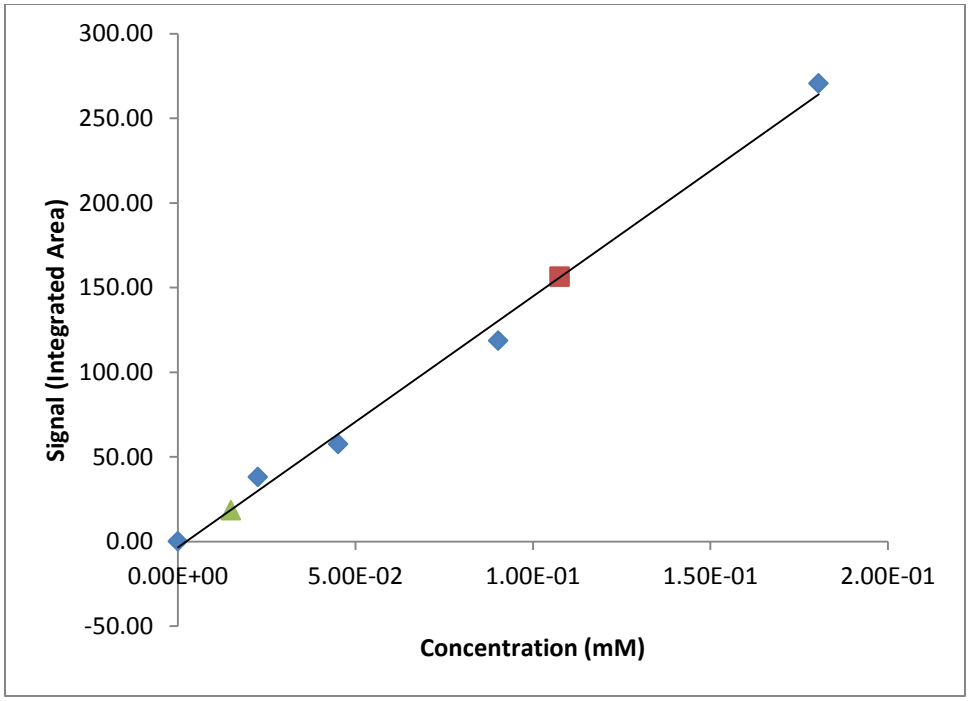

Figure S1. Spin counting to quantify concentration of tyrosyl radical formed in F33Y-Cu_BMb after reaction with H_2O_2 or O_2. Data points from TEMPO standards are in blue square, point from F33Y-Cu_BMb reacted with H_2O_2 is in red square and that from ferrous F33Y-Cu_BMb with O_2 is in green triangle. Standard curve (black line) is drawn based on TEMPO standards.

Table S1. Spin counting of standard TEMPO solution and radical from F33Y-Cu_BMb. R=0.99956

Labeled Concentration/mM	Actual Concentration/mM	Gain	Area	Area/Gain
1	0.9	400	6.17×10^5	1542.09
0.2	0.18	2000	5.41×10^5	270.57
0.1	0.090	4000	4.74×10^5	118.53
0.05	0.045	8000	4.60×10^5	57.53
0.025	0.023	12500	4.75×10^5	38.01
0	0			0.00
F33Y-Cu_BMb+H_2O_2	0.11	4000	6.26×10^5	156.39
ferrous F33Y-Cu_BMb+O_2	0.015	12500	2.29×10^5	18.32

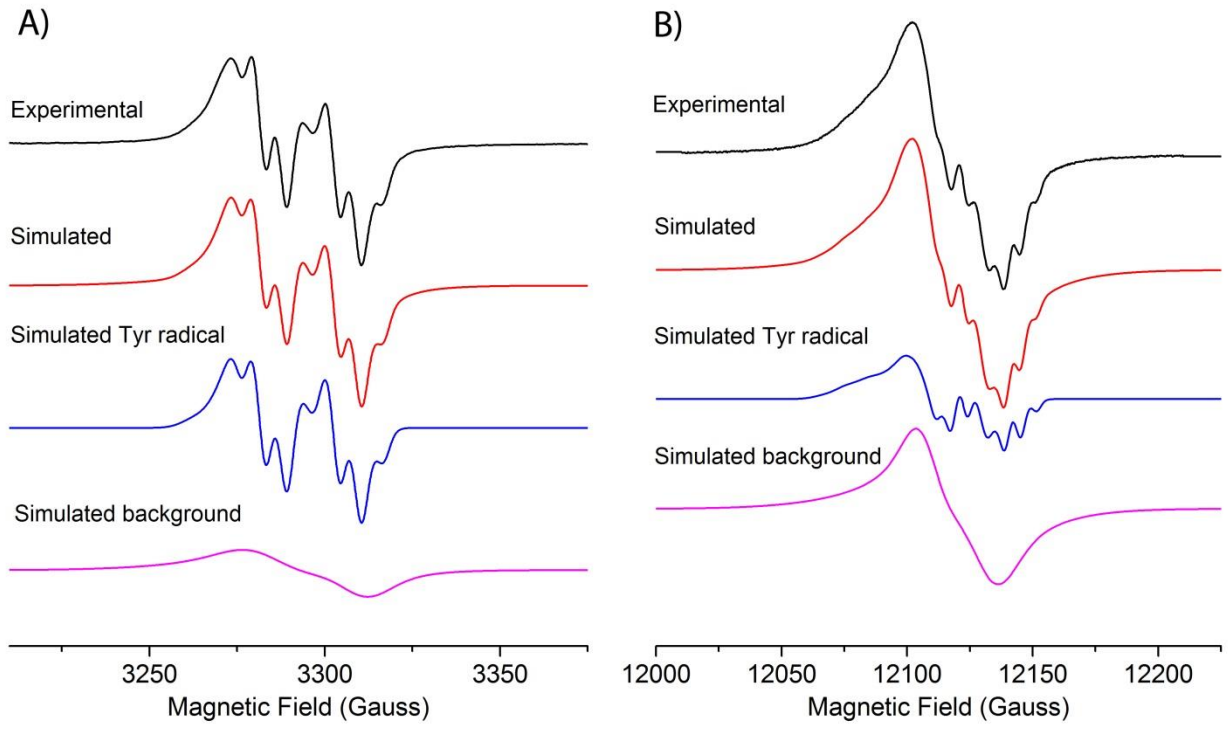

Figure S2. X-band (A) and Q-band (B) EPR spectra of H_2O_2-reacted F33Y-Cu_BMb, showing experimental spectra (black), simulated spectra (red), simulated tyrosyl radical species (blue) and background species (magenta).

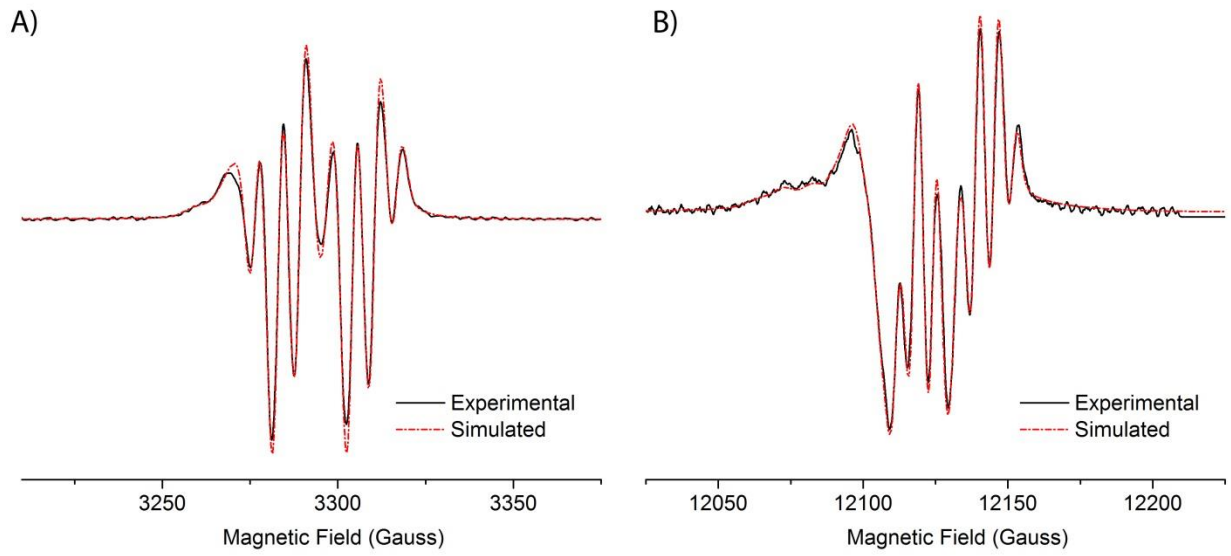

Figure S3. Second derivatives of X-band (A) and Q-band (B) spectra of F33Y-Cu_BMb after H_2O_2 treatment. Experimental spectra were in black solid line while simulated spectra were in red dashed line. The secondary derivatives are more sensitive to the species with well-resolved hyperfine structure. The good agreement between experimental and simulated spectra indicates the Tyr radical-like species is modeled well.

Table S2. Simulated EPR parameters for tyrosyl radical in H_2O_2-reacted F33Y-Cu_BMb

	species	fraction	g_x	g_y	g_z
X-band	Tyr radical	0.53	2.0091	2.0044	2.0021
	background	0.47	2.0110	2.0118	1.9938
Q-band	Tyr radical	0.29	2.0091	2.0044	2.0021
	background	0.71	2.0060	2.0056	2.0018

	species	W_x/Gauss	W_y/Gauss	W_z/Gauss	Δg_x	Δg_y	Δg_z
X-band	Tyr radical	7.5	4.7	3.2	0.0005	0.0001	0.0000
	background	16.0	55.0	11.7			
Q-band	Tyr radical	7.5	4.7	3.2	0.0005	0.0001	0.0000
	background	11.5	76.7	14.4			

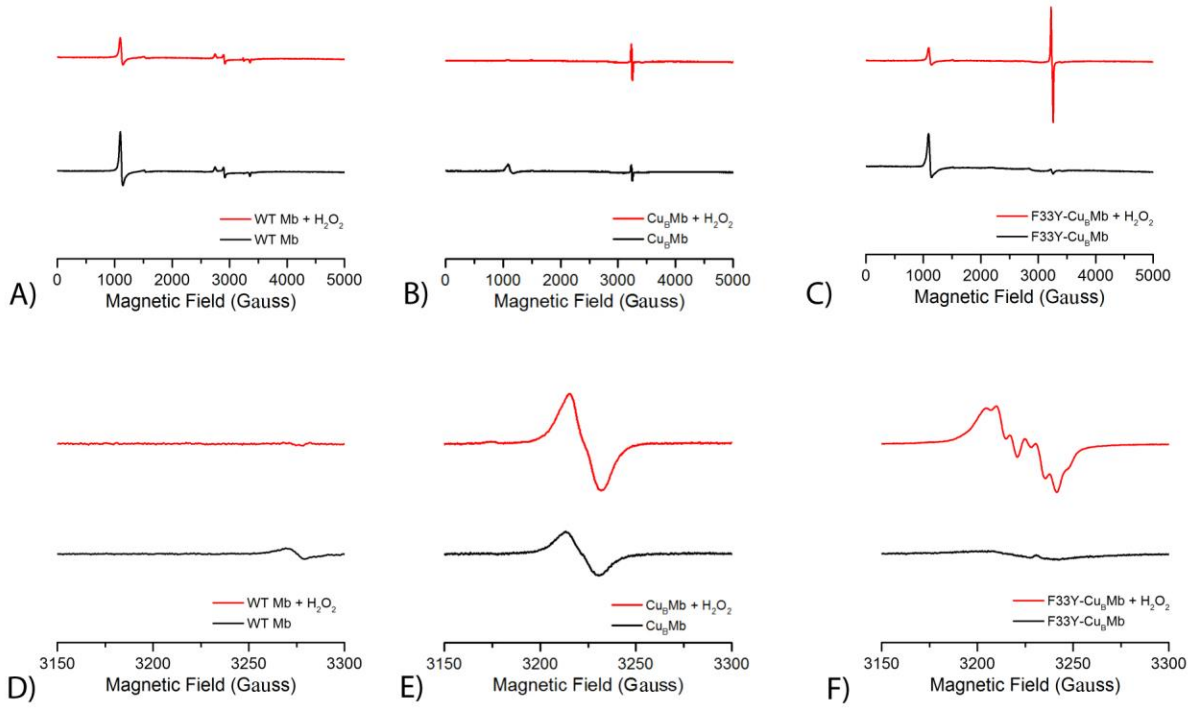

Figure S4. X-band EPR spectra of WT Mb, Cu_BMb and F33Y-Cu_BMb in absence (black line) and in presence(red line) of 1 Eq. H_2O_2. A) and D) are WT Mb; B) and E) are Cu_BMb; C) and F) are F33Y-Cu_BMb. In top lane are spectra taken over 5000 Gauss. Experiment parameters: frequency: 9.05 GHz; power: 5 mW; gain: 2000; temperature: 30K; modulation: 10 Gauss. In bottom lane are spectra taken over 150 Gauss. Experiment parameters: frequency: 9.05 GHz; power: 2 mW; gain: 4000-12500; temperature: 30K;

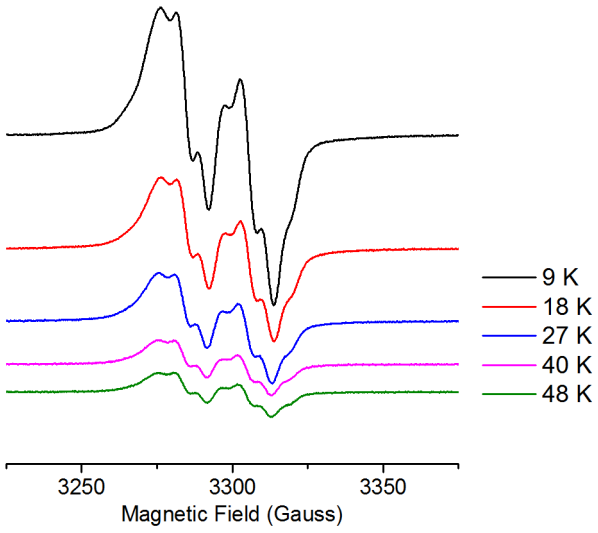

modulation: 4 Gauss.

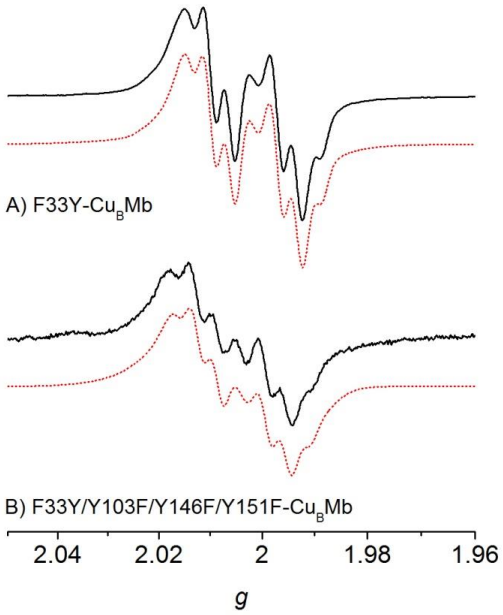

Figure S5. Experimental (black) and simulated (red) EPR spectra of A) F33Y-Cu_BMb and B) F33Y/Y103F/Y146F/Y151F-Cu_BMb after H_2O_2 treatment. Experiment parameters: frequency: 9.05 GHz; power: 2 mW; gain: 2000 for F33Y-Cu_BMb and 12500 for F33Y/Y103F/Y146F/Y151F-Cu_BMb; temperature: 30K; modulation: 4 Gauss.

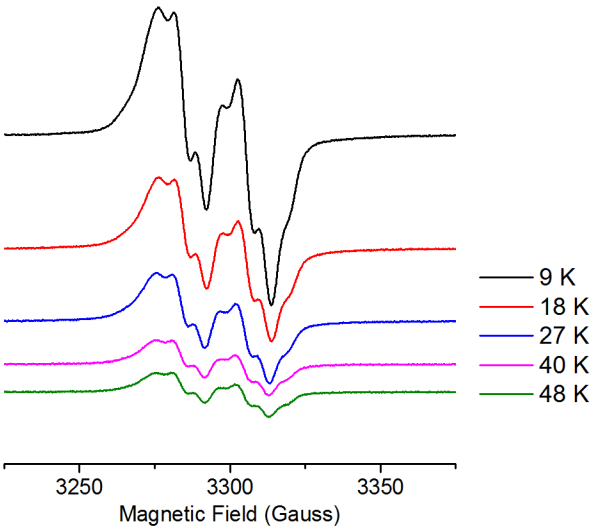

Figure S6. EPR spectra of the same F33Y-Cu_BMb after reaction with H_2O_2 recorded at various temperatures. Microwave frequency: 9.23 GHz; power: 0.2 mW; gain: 4000; temperature: 30K; modulation: 2 Gauss.

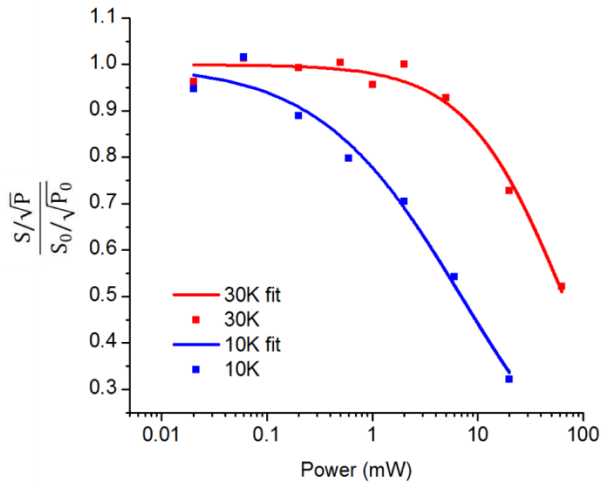

Figure S7. Plot of relative signal vs. power and fitting for power saturation experiment at 10K (blue) and 30K (red). The half saturation power is calculated to be 10 mW at 10 K and 67 mW at 30 K.

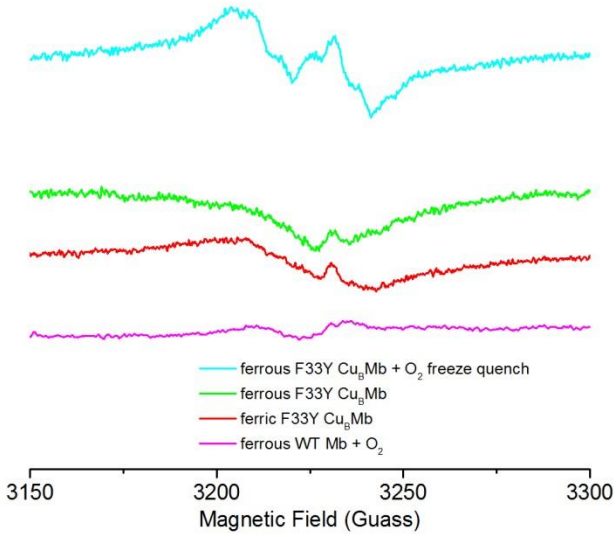

Figure S8. EPR spectra of ferrous F33Y-Cu_BMb with or without treatment of O_2, ferric F33Y-Cu_BMb and O_2 bound WT Mb. Experiment parameters for X-band EPR: frequency: 9.05 GHz; power: 2 mW; gain: 12500; temperature: 30K; modulation: 4 Gauss.

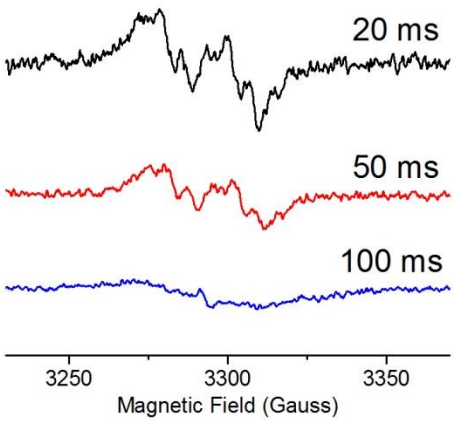

Figure S9. EPR spectra of F33Y-Cu_BMb reacted with O_2 and quenched at 20 ms, 50 ms and 100 ms. Experiment parameters for X-band: frequency: 9.23 GHz; power: 2 mW; gain: 25000; temperature: 30K; modulation: 2 Gauss.

References

(1) Sigman, J. a.; Kwok, B. C.; Lu, Y. *J. Am. Chem. Soc.* **2000**, *122*, 8192.
(2) Miner, K. D.; Mukherjee, A.; Gao, Y.-G.; Null, E. L.; Petrik, I. D.; Zhao, X.; Yeung, N.; Robinson, H.; Lu, Y. *Angew. Chem., Int. Ed.* **2012**, *51*, 5589.
(3) Nilges, M. J.; Matteson, K.; Bedford, R. L. In *ESR Spectroscopy in Membrane Biophysics*; Hemminga, M. A., Berliner, L., Eds.; Springer: New York, 2007; Vol. 27.
(4) Yu, Y. G.; Thorgeirsson, T. E.; Shin, Y.-K. *Biochemistry* **1994**, *33*, 14221.